ELSEVIER Applied Mathematics and Computation 107 (2000) 27–55

APPLIED MATHEMATICS AND COMPUTATION

www.elsevier.nl/locate/amc

Generalised solutions, discrete models and energy estimates for a 2D problem of coupled field theory

R.V.N. Melnik [1]

Mathematical Modelling and Numerical Analysis Group, Department of Mathematics and Computing, University of Southern Queensland, Toowoomba QLD 4350, Australia

Abstract

In this article the author constructs an effective difference scheme for the solution of coupled dynamic electroelasticity problems for finite-dimensional solids. Such a construction is based on the energy conservation law for the electromechanical system and the definition of generalised solutions for the corresponding differential problem. Results of computational experiments are presented for hollow piezoceramic cylinders in the two-dimensional case. © 2000 Elsevier Science Inc. All rights reserved.

Keywords: Piezoelectrics; Discrete conservation laws for coupled systems; Electro–mechanical interactions; Generalised solutions

1. Introduction: Piezoceramic applications and coupled field theory

Piezoelectricity is an example of phenomena where coupling two physical fields of different natures (namely mechanical and electrical fields) is a key factor to be taken into account in a variety of applications. It is just one of many important examples where two theories, originally developed independently of each other (in this case the theory of elasticity and the Maxwell theory of electromagnetic waves), have to be considered in intrinsic correlation. Such examples are usually assigned to the domain of coupled field theory.

[1] Tel.: +61 7 46312 632; fax: +61 7 463 11775; e-mail: melnik@usq.edu.au.

PII: S0096-3003(98)10143-1

Discovered in 1880 by the Curies, piezoelectricity has essentially contributed to technological advances. Since the time of Langevin's sonar emitter, more and more devices and functional components are being based on piezoelectrics. The development of new piezoelectric material has echoed in the rapid growth in many industrial applications including telecommunications, consumer electronics and many other areas. Piezoelectricity has been put on a rigorous mathematical basis by classical works of Voigt, Mindlin, Tiersten, Mason, Maugin, Ulitko, Nowacki and many other researchers (see Refs. [2,3,10,13,26,27]).

One of the first piezoelectric material that deserved a lot of attention from engineers and designers was the lead-zirconate-titanate (PZT) piezoceramic (and its derivatives). The PZT-family of piezoelectrics has a number of important properties, such as moderate temperature range, resistance to mechanical and electrical stress-induced depolarisation, large piezoelectric coefficients [9]. Of course, it would be proper to say that ceramics have been always a part of human life. However active applications of ceramic materials began just about six decades ago. Later, in the 1950s, piezoceramics started being widely employed for industrial purposes.

By now it is technologically possible (for example, by doping of PZT ceramics) to achieve many useful properties of piezoceramics such as, a high surface coupling coefficient, a low temperature coefficient of delay time and others. As a result, doped piezoceramics have become very important in many high temperature, high frequency device applications. For example, piezoceramic substrates are widely used for surface acoustic wave (SAW) applications including filters and biological/chemical sensors [8]. Piezoceramic is an intrinsic part in many ultrasonic transducer elements for nondestructive material evaluation, infrared sensors, hydrophones, medical diagnostics etc. An important aspect of new piezoceramic applications is that new technologies become more ecologically friendly. For new families of piezoceramics (including those with bismuth perovskites), the atmosphere control over the lead-induced evaporation is either not necessary, or can be minimised. Another advantage of new piezoceramics is due to their properties under a large level of vibrations for high-power piezoelectric devices (such as piezoelectric actuators or ultrasonic motors). Indeed, in many applications, one has to confront the problem of heat generation and subsequent changes in piezoelectric properties which is difficult to solve for classical piezoceramics (for example, due to the lead loss in PZT-based piezoceramics) [31].

In many applications PZT-based ceramics remain the most extensively used piezoelectric material. Amongst many other advantages it is cheap and easy to fabricate. During the last few decades piezoelectric polymers have become an alternative material. There are applications (such as hydrophone design) where it is important to have a higher acoustic match between ceramics and the transmitting media as well as to be able to form curved surfaces [12]. In the latter cases the use of piezoelectric polymers (such as Polyvinylidene Fluoride (PVDF) and its copolymers with trifluoroethylene) is quite successful [4]. In addition, many piezoceramic polymers have a high electrical conductivity and are being widely used in many technical devices, including those in laser and infrared technologies. However, the main problems with polymers lie with, typically, a low dielectric constant, relatively high cost of fabrication and a low electromechanical coupling. Therefore many technological advances are connected with the use of composites based on the PZT-ceramics which have a high thermal stability and many other useful properties. Some piezoelectric ceramic/polymer composites have a great future potential to replace classical piezoceramics and piezopolymers. In many cases such composites are not difficult to fabricate, for example, by embedding of PZT rods in a polymer/copolymer matrix.

Recent interest in smart structures has once again reemphasized the importance of rigorous mathematical tools in a better understanding of the electroelastic behaviour of piezoceramics as an integral part of structures [23].

In a large number of the applications discussed above, it is important to have quantitative characteristics of the electroelastic behaviour of finite-dimensional solids in the dynamic, rather than in the stationary, regime taking into account the influence of electric and mechanical fields onto each other. The quantitative understanding of the effect produced by the coupling of electrical and mechanical field is essential to the successful design of components and devices [6]. However, analytical solutions for coupled problems of piezoelectricity are limited. This is especially true for the nonstationary case. As a consequence, numerical methods become the most natural and effective tool of research in coupled field theory in general, and in piezoelectricity in particular [1,5,14–19,21,22,24,25,33].

In this paper we consider a two-dimensional, nonstationary model for the description of coupled electromechanical fields in piezoceramic materials. We give a rigorous mathematical derivation of an effective numerical method for the investigation of such fields in finite-length hollow piezoceramic cylinders. The article is organised in five sections. Section 2 is concerned with the main notation used throughout of the paper. In Section 3 we consider the mathematical model of coupled dynamic electroelasticity in the 2D case and discuss the main approaches for its treatment. Section 4 deals with the energy balance equation for the piezoelectric body. Such an equation is derived from the definition of the generalised solution of the original differential problem. In Section 5 we construct the difference scheme from the energy balance equation. Section 6 addresses the important issues of boundedness of the energy operator for the differential model. The results of computational experiments are presented in Section 7.

2. Notation

The following notations are used throughout this paper

- $\bar{Q}_T = \bar{G} \times \bar{I}$ where
$$\bar{G} = \{(r,z)\colon\ R_0 \leqslant r \leqslant R_1,\ Z_0 \leqslant z \leqslant Z_1\},\ \ \bar{I} = \{t\colon\ 0 \leqslant t \leqslant T\}$$
is the space-time region of interest;
- u_r and u_z are components of the displacement vector;
- ϕ is the electric field potential;
- $f_i(r,z,t),\ i = 1,2$ are components of the vector of mass forces;
- $f_3(r,z,t)$ is the function of volume charges;
- ρ is the density of the piezoceramic material;
- E_r and E_z are vector components of the stress of electric field;
- D_r and D_z are vector components of electric induction;
- σ_r, σ_θ, σ_z and σ_{rz} are components of the field of stresses;
- c_{kl} tensor components of elastic quantities;
- e_{ij} tensor components of electro-elastic quantities;
- c_{kl} tensor components of electric quantities;
- $\bar{\omega}_{h\tau} = \bar{\omega}_h \times \bar{\omega}_\tau$ is the difference grid that covers the space-time region Q_T;
- $\bar{\omega}_h = \bar{\omega}_{h_1} \times \bar{\omega}_{h_2}$;
- $\bar{\omega}_{h_1} = \{r_i\colon\ r_i = R_0 + ih_1,\ i = 0,1,\ldots,N,\ h_1 = (R_1 - R_0)/N\}$ is the r-direction difference grid;
- $\bar{\omega}_{h_2} = \{z_j\colon\ z_j = Z_0 + jh_2,\ j = 0,1,\ldots,M,\ h_2 = (Z_1 - Z_0)/M\}$ is the z-direction difference grid;
- $\bar{\omega}_\tau = \{t_k\colon\ t_k = k\tau,\ \tau = T/L,\ k = 0,1,\ldots,L\}$ is the temporal grid;
- "flux" nodes are introduced as
$$\bar{r} = r - h_1/2,\ \bar{z} = z - h_2/2.$$
(in these nodes we define deformations and stresses);
- $\omega_{h_1} = \{r_i = R_0 + ih_1,\ i = 1,\ldots,N-1\}$, $\omega^+_{h_1} = \{r_i = R_0 + ih_1,\ i = 1,\ldots,N\}$, $\omega^-_{h_1} = \{r_i = R_0 + ih_1,\ i = 0,\ldots,N-1\}$ are auxiliary grids (in a similar way we define grids $\omega_{h_2}, \omega^+_{h_2}, \omega^-_{h_2}$);
- $\gamma_1 = \{(r,z)\colon\ R_0 < r < R_1, z = Z_0\}$, $\gamma_2 = \{(r,z)\colon\ R_0 < r < R_1,\ z = Z_1\}$, $\gamma_3 = \{(r,z)\colon\ r = R_0,\ Z_0 < z < Z_1\}$, $\gamma_4 = \{(r,z)\colon\ r = R_1,\ Z_0 < z < Z_1\}$ are the boundaries of the spatial region G;
- $\gamma_{13} = \{r = R_0, z = Z_0\}$, $\gamma_{23} = \{r = R_0, z = Z_1\}$, $\gamma_{24} = \{r = R_1, z = Z_1\}$, $\gamma_{14} = \{r = R_1, z = Z_0\}$ are the vertices (corner points) of the region G.
We use the standard notation for difference derivatives of a function $y(r,z,t)$ defined on the grid $\bar{\omega}_{h\tau}$ [22,28–30]. For example,
- $y_r = (y(r + h_1, z, t) - y(r,z,t))/h_1$ denotes the forward difference derivative in the r-direction;
- $y_{\bar{r}} = (y(r,z,t) - y(r - h_1, z, t))/h_1$ denotes the backward difference derivative in the r-direction;

- $y_{\bar{r}r} = (y(r+h_1,z,t) - 2y(r,z,t) + y(r-h_1,z,t))/h_1^2$ is the second ("central") difference derivative in the r-direction.

In a similar manner we define difference derivatives in the z-direction and the derivatives with respect to t.

3. Mathematical models of coupled dynamic electroelasticity

Mathematically, the process of propagation of axially symmetric electroelastic waves in hollow finite-length piezoceramic cylinders with radial preliminary polarisation, can be described by a coupled system of partial differential equations which include

- the equations of motion of the piezoelectric medium in cylindrical coordinates

$$\rho \frac{\partial^2 u_r}{\partial t^2} = \frac{\partial \sigma_r}{\partial r} + \frac{\partial \sigma_{rz}}{\partial z} + \frac{\sigma_r - \sigma_\theta}{r} + f_1, \tag{1}$$

$$\rho \frac{\partial^2 u_z}{\partial t^2} = \frac{\partial \sigma_{rz}}{\partial r} + \frac{\partial \sigma_z}{\partial z} + \frac{\sigma_{rz}}{r} + f_2, \tag{2}$$

- the Maxwell equation for piezoelectrics (in the acoustic range of frequencies, it is the forced electrostatic equation of dielectrics)

$$\frac{1}{r}\frac{\partial}{\partial r}(rD_r) + \frac{\partial D_z}{\partial z} = f_3, \tag{3}$$

- and, state equations for piezoceramic with radial preliminary polarisation

$$\begin{aligned}
&\sigma_r = c_{33}\epsilon_r + c_{13}(\epsilon_\theta + \epsilon_z) - e_{33}E_r,\ \sigma_\theta = c_{13}\epsilon_r + c_{11}\epsilon_\theta + c_{12}\epsilon_z - e_{13}E_r,\\
&\sigma_z = c_{13}\epsilon_r + c_{12}\epsilon_\theta + c_{11}\epsilon_z - e_{13}E_r,\ \sigma_{rz} = c_{44}\epsilon_{rz} - e_{15}E_z,\\
&D_r = e_{33}\epsilon_r + e_{13}(\epsilon_\theta + \epsilon_z) + \epsilon_{33}E_r,\ D_z = 2e_{15}\epsilon_{rz} + \epsilon_{11}E_z
\end{aligned} \tag{4}$$

(or state equations for piezoceramic with circular preliminary polarisation [3,25]).

The function of electrostatic potential is introduced by the formulae

$$E_r = -\frac{\partial \varphi}{\partial r}, \qquad E_z = -\frac{\partial \varphi}{\partial z} \tag{5}$$

and the relationship between deformations and displacements (Cauchy relationships) have the form

$$\epsilon_r = \frac{\partial u_r}{\partial r}, \quad \epsilon_\theta = \frac{u_r}{r}, \quad \epsilon_z = \frac{\partial u_z}{\partial z}, \quad \epsilon_{rz} = \frac{1}{2}\left(\frac{\partial u_r}{\partial z} + \frac{\partial u_z}{\partial r}\right). \tag{6}$$

The system (1)–(6) is considered in the space-time region Q_T and is complemented by the following initial conditions

$$u_r(r,z,0) = u_r^{(0)}(r,z), \quad \frac{\partial u_r(r,z,0)}{\partial t} = u_r^{(1)}(r,z), \tag{7}$$

$$u_z(r,z,0) = u_z^{(0)}(r,z), \qquad \frac{\partial u_z(r,z,0)}{\partial t} = u_z^{(1)}(r,z) \tag{8}$$

with known functions $u_r^{(i)}$, $u_z^{(i)}$, $i = 1,2$.

Mechanical boundary conditions for this problem have the form

$$\sigma_r(R_i,z,t) = p_r^{(i)}(z,t),\ \sigma_z(r,Z_i,t) = p_z^{(i)}(r,t), \quad i = 0,1, \tag{9}$$

$$\sigma_{rz}(R_i,z,t) = p_{zt}^{(i)}(z,t),\ \sigma_{rz}(r,Z_i,t) = p_{rt}^{(i)}(r,t), \quad i = 0,1, \tag{10}$$

where $p_r^{(i)}$, $p_z^{(i)}$, $p_{zt}^{(i)}$, $p_{rt}^{(i)}$, $i = 0,1$ are given functions.

Finally, the formulation of electric boundary conditions depends on the character of the electric loading and the location of electrodes on the body surface. We assume that lateral surfaces of the cylinder are covered by infinitely thin short circuiting electrodes, and that the dielectric permittivity of the surrounding media is much less than the dielectric permittivity of ceramics (this is of course true for both vacuum and air). Then we have

$$\varphi(R_i,z,t) = 0, \quad D_z(r,Z_i,t) = 0, \quad i = 0,1. \tag{11}$$

The assumption of homogeneity of electric boundary conditions made in Eq. (11) does not restrict generality of the model. Indeed problems with non-homogeneous conditions can be reduced to homogeneous ones using the procedure described in Ref. [22].

In the general case, the determination of electric field in a piezoelectric body has to be performed simultaneously with the determination of its deformation. In other words, a consistent solution of system (1)–(3) has to be found with corresponding mechanical and electrical boundary conditions defined by Eqs. (9)–(11), state Eq. (4) and initial conditions (7), (8).

In its essence, the solution of Eqs. (1)–(11) represents mixed electroelastic waves. The coupling of electric and elastic components in a unified electroelastic field and the necessity of dealing with nonstationary rather than steady-state situations lead to major difficulties in the rigorous investigation of behaviour of piezoceramic-based solids. For dynamic problems of coupled field theory in general, and for piezoelectricity in particular, numerical methods become the natural and efficient way of problem solution. Amongst the numerical techniques effectively used in this field are: Finite Element Approach (FEM) [1,5,14,15,17,18], Boundary Element Method (BEM) [16,19,33] and Method of Finite Differences (FDM) [21,22,24,25]. The latter method is very attractive since it can be readily applied to practically any system of differential equations that is especially important in coupled field theory. In addition, FDM enjoys many of the advantages present in FEM and BEM provided the differential problem is reformulated in a variational form. Such a reformulation for mathematical models of piezoelectricity goes back to Mindlin's works (see references in Refs. [3,22]). Of course, the existence of physical conservation laws for a physical quantity is closely connected with the description of a system using variational principles. Therefore, one of the features of models for electroelasticity that is desirable to transfer to a difference scheme, is their original variational properties. An effective way to construct such difference schemes, is the method of approximation of variational functional [28–30].

From the mathematical point of view, the most natural way of variational reformulation of the differential problem, is based on the concept of generalised solutions. Such a reformulation puts us closer to the real practical situations where solutions may not be smooth in the classical sense. For coupled dynamic piezoelectricity, this idea was first applied by the author of this article and his collaborators in the one-dimensional case (see [22] and references therein). Effective difference schemes for infinite-length hollow piezoceramic cylinders were constructed and investigated in Refs. [22,24]. In Ref. [20] a theory of existence and uniqueness for generalised solutions of the associated mathematical models was developed. In this paper we deal with the modelling of finite-length cylinders.

4. Generalised solutions of coupled electroelasticity and the energy balance equation

The solution of problem (1)–(11) will be understood in the following sense.

Definition 4.1 ([21]). The triple of functions

$$(u_r(r,z,t), u_z(r,z,t), \varphi(r,z,t)) \in \left[W_2^1(Q_T)\right]^2 \times L_2\left(I, \overset{0}{W}{}_2^1(G)\right)$$

such that for $t = 0$ $u_r(r,z,t) = u_r^{(0)}(r,z)$ and $u_z(r,z,t) = u_z^{(0)}(r,z)$ is called the generalised solution of the coupled dynamic problem electroelasticity (1)–(11) if it satisfies the following identities

$$\begin{aligned}
&\int_{Q_T} r\left(-\rho\frac{\partial u_r}{\partial t}\frac{\partial \eta_1}{\partial t} + \sigma_r\frac{\partial \eta_1}{\partial r} + \frac{\sigma_\theta}{r}\eta_1 + \sigma_{rz}\frac{\partial \eta_1}{\partial z}\right) \mathrm{d}r\,\mathrm{d}z\,\mathrm{d}t \\
&- \int_G r\rho u_r^{(1)}(r,z)\eta_1(r,z,0)\,\mathrm{d}r\,\mathrm{d}z \\
&= \int_{Q_T} r f_1 \eta_1\,\mathrm{d}r\,\mathrm{d}z\,\mathrm{d}t \quad \forall \eta_1 \in \hat{W}{}_2^1(Q_T),
\end{aligned} \tag{12}$$

$$\int_{Q_T} r\left(-\rho \frac{\partial u_z}{\partial t}\frac{\partial \eta_2}{\partial t} + \sigma_{rz}\frac{\partial \eta_2}{\partial r} + \sigma_z \frac{\partial \eta_2}{\partial z}\right) \mathrm{d}r\,\mathrm{d}z\,\mathrm{d}t$$

$$- \int_G r\rho u_z^{(1)}(r,z)\eta_2(r,z,0)\,\mathrm{d}r\,\mathrm{d}z$$

$$= \int_{Q_T} rf_2\eta_2\,\mathrm{d}r\,\mathrm{d}z\,\mathrm{d}t \quad \forall \eta_2 \in \hat{W}_2^1(Q_T), \tag{13}$$

$$\int_G rD_r \frac{\partial \zeta}{\partial r}\,\mathrm{d}r\,\mathrm{d}z - \int_G r\frac{\partial D_z}{\partial z}\frac{\partial \zeta}{\partial z}\,\mathrm{d}r\,\mathrm{d}z$$

$$= \int_G rf_3\zeta\,\mathrm{d}r\,\mathrm{d}z \quad \forall \zeta \in \overset{0}{W}{}_2^1(G) \text{ and for a.e. } t \in (0,T). \tag{14}$$

The metric space $\hat{W}_2^1(Q_T)$, used in the definition, consists of such elements of $W_2^1(Q_T)$ which equal zero at $t = T$, and the space $\overset{0}{W}{}_2^1(G)$ consists of such elements of $W_2^1(G)$ which equal zero for $r = R_0, R_1$.

The existence and uniqueness of generalised solutions for the model (1)–(11) was investigated in Ref. [21] where the following theorem was proved.

Theorem 4.1. *If*

$$f_i \in W_2^1(I,H), \quad i = 1,2, \qquad \frac{\partial f_3}{\partial t} \in L_2\left(I, \left(\overset{0}{W}{}_2^1(G)\right)^*\right),$$

$$f_3|_{t=0} \in \left(\overset{0}{W}{}_2^1(G)\right)^*, \quad u_r^{(0)}, u_z^{(0)} \in W_2^1(G), \quad u_r^{(1)}, u_z^{(1)} \in L_2(G),$$

then there exists a unique generalised solution of the problem (1)–(11) *with the following properties*

$$\frac{\partial u_r}{\partial t}, \frac{\partial u_z}{\partial t} \in L_2(I,H), \qquad \frac{\partial^2 u_r}{\partial t^2}, \frac{\partial^2 u_z}{\partial t^2} \in L_2\big(I, (W_2^1)^*\big), \qquad \frac{\partial \varphi}{\partial t} \in L_2\left(I, (\overset{0}{W}{}_2^1)^*\right),$$

where the star denotes a dual space, and $H = L_2(G)$.

This result is central to the construction of effective numerical schemes for the solution of problem (1)–(11). Indeed, two of the key elements of the proof of Theorem 4.1, is the application of the Faedo–Galerkin procedure and the obtaining the representation for the energy operator. The later may be derived from Definition 4.1 by choosing appropriate trial functions η_1, η_2 and ζ in Eqs. (12)–(14). We will not concentrate here on this procedure, and refer the reader to Ref. [22], where such a procedure was explained for one-dimensional models. The final result is as follows

$$\frac{d\mathscr{E}}{dt} = \int\int_{\Omega} r\left[\frac{\partial D_r}{\partial t}E_r + \frac{\partial D_z}{\partial t}E_z\right] d\Omega + \int_{R_0}^{R_1} r\left[\sigma_{rz}\frac{\partial u_r}{\partial t} + \sigma_z\frac{\partial u_z}{\partial t}\right] dr\Bigg|_{Z_0}^{Z_1}$$
$$+ \int_{Z_0}^{Z_1} r\left[\sigma_r\frac{\partial u_r}{\partial t} + \sigma_{rz}\frac{\partial u_z}{\partial t}\right] dz\Bigg|_{R_0}^{R_1} + \int\int_{\Omega} r\left[f_1\frac{\partial u_r}{\partial t} + f_2\frac{\partial u_z}{\partial t}\right] d\Omega, \qquad (15)$$

where the total inner energy of the system, $\mathscr{E} = K + W + P$, consists of the three coupled parts

- kinetic energy of the system

$$K = \frac{\rho}{2}\int\int_{\Omega} r\left\{\left(\frac{\partial u_r}{\partial t}\right)^2\left(\frac{\partial u_z}{\partial t}\right)^2\right\} d\Omega,$$

- the energy of elastic deformation

$$W = \frac{1}{2}\int\int_{\Omega} r\{c_{33}\epsilon_r^2 + c_{11}(\epsilon_\theta^2 + \epsilon_z^2) + 2c_{13}(\epsilon_\theta\epsilon_r + \epsilon_z\epsilon_r)$$
$$+ 2c_{12}\epsilon_z\epsilon_\theta + 2c_{44}\epsilon_{rz}^2\} d\Omega,$$

- and the energy of electric field

$$P = \frac{\epsilon_{33}}{2}\int\int_{\Omega} rE_r^2 \, d\Omega + \frac{\epsilon_{11}}{2}\int\int_{\Omega} rE_z^2 \, d\Omega.$$

The energy conservation law Eq. (15) derived for the coupled system described by the model (1)–(11), is fundamental to the investigation of system stability. One of the key factors of such investigations includes establishing some bounds on the energy functional $\mathscr{E}(t)$ at any given moment of time. Ultimately, it is such bounds that allow us to guarantee the stability of corresponding difference problems under certain constraints on time and space discretisations.

In Section 5 we use the energy conservation law Eq. (15) in order to construct effective difference schemes for the solution of problem (1)–(11).

5. Derivation of numerical schemes from the conservation laws for coupled systems

Let $\tilde{u}_1 \equiv \tilde{u}_1(r,z,t)$, $\tilde{u}_2 \equiv \tilde{u}_2(r,z,t)$, $\tilde{\varphi} \equiv \tilde{\varphi}(r,z,t)$ be the functions of discrete variables $r \in \bar{\omega}_{h_1}$, $z \in \bar{\omega}_{h_2}$ and continuous variable $t \in \bar{I} \equiv \{t: 0 \leqslant t \leqslant T\}$, that give approximations to u_r, u_z and φ respectively. Then we denote

$$\tilde{u}_1^{(\pm 1_r)} = \tilde{u}_1(r \pm h_1, z, t), \; \tilde{u}_2^{(\pm 1_z)} = \tilde{u}_2(r, z \pm h_2, t),$$

$$\tilde{u}^{(\pm 1, \pm 1)} = \tilde{u}(r \pm h_1, z \pm h_2, t),$$

$$\tilde{\epsilon}_r = \frac{1}{2}\left((\tilde{u}_1)_{\bar{r}} + \left(\tilde{u}_1^{(-1_z)}\right)_{\bar{r}}\right), \quad \tilde{\epsilon}_\theta = \frac{1}{4\bar{r}}\left(\tilde{u}_1 + \tilde{u}_1^{(-1_r)} + \tilde{u}_1^{(-1_z)} + \tilde{u}_1^{(-1,-1)}\right),$$

$$\tilde{\epsilon}_z = \frac{1}{2}\left((\tilde{u}_2)_{\bar{z}} + \left(\tilde{u}_2^{(-1_r)}\right)_{\bar{z}}\right), \quad 2\tilde{\epsilon}_{rz} = \frac{1}{2}\left((\tilde{u}_1)_{\bar{z}} + \left(\tilde{u}_1^{(-1_r)}\right)_{\bar{z}} + (\tilde{u}_2)_{\bar{r}} + \left(\tilde{u}_2^{(-1_z)}\right)_{\bar{r}}\right),$$

$$\tilde{E}_r = -\frac{1}{2}\left(\tilde{\varphi}_{\bar{r}} + \left(\tilde{\varphi}^{(-1_z)}\right)_{\bar{r}}\right), \quad \tilde{E}_z = -\frac{1}{2}\left(\tilde{\varphi}_{\bar{z}} + \left(\tilde{\varphi}^{(-1_r)}\right)_{\bar{z}}\right).$$

Similar to the one-dimensional case (see details in Ref. [22]), the construction of the difference scheme for the solution of problems (1)–(11) is based on the obtaining a difference analogue of the energy conservation law. The procedure for the construction may be split into two stages [25,21]:

- first, using the method of approximation of quadratic functional of energy, we perform discretisation in space,
- then, the differential-difference scheme obtained on the first stage is discretised in time.

Below, we consider these stages in some detail.

The integral of kinetic energy is approximated by the following quadrature formula

$$K^h = \frac{\rho}{2}\sum_{\bar{\omega}_h} r\hbar_1\hbar_2\left[\left(\frac{\mathrm{d}\tilde{u}_1}{\mathrm{d}t}\right)^2 + \left(\frac{\mathrm{d}\tilde{u}_2}{\mathrm{d}t}\right)^2\right] \tag{16}$$

(where $\hbar_\alpha = h_\alpha/2$ when $r \in \bar{\omega}_{h_\alpha}/\omega_{h_\alpha}$ and $\hbar_\alpha = h_\alpha$ when $r \in \omega_{h_\alpha}$, $\alpha = 1, 2$), and the integrals of elastic deformation and electric field by

$$W^h + P^h = \frac{1}{2}\sum_{\omega_h^+}\bar{r}h_1h_2\Big[c_{33}\tilde{\epsilon}_r^2 + c_{11}(\tilde{\epsilon}_\theta^2 + \tilde{\epsilon}_z^2) + 2c_{13}(\tilde{\epsilon}_\theta + \tilde{\epsilon}_z)\tilde{\epsilon}_r + 2c_{12}\tilde{\epsilon}_z\tilde{\epsilon}_\theta + 2c_{44}\tilde{\epsilon}_{rz}^2 + \epsilon_{33}\tilde{E}_r^2 + \epsilon_{11}\tilde{E}_z^2\Big]. \tag{17}$$

We note that if the solution of the problems (1)–(11) is from $[W_2^4(Q_T)]^2 \times L^2(I, W_2^4(G))$, then the quadrature formulas (16) and (17) are formulas of the second order accuracy in $|h| = (h_1^2 + h_2^2)^{1/2}$.

Taking into account differential–difference analogues of state equations

$$\begin{aligned}
&\tilde{\sigma}_r = c_{33}\tilde{\epsilon}_r + c_{13}(\tilde{\epsilon}_\theta + \tilde{\epsilon}_z) - e_{33}\tilde{E}_r,\ \tilde{\sigma}_\theta = c_{13}\tilde{\epsilon}_r + c_{11}\tilde{\epsilon}_\theta + c_{12}\tilde{\epsilon}_z - e_{13}\tilde{E}_r,\\
&\tilde{\sigma}_z = c_{13}\tilde{\epsilon}_r + c_{12}\tilde{\epsilon}_\theta + c_{11}\tilde{\epsilon}_z - e_{13}\tilde{E}_r,\ \tilde{\sigma}_{rz} = c_{44}\tilde{\epsilon}_{rz} - e_{15}\tilde{E}_z,\\
&\tilde{D}_r = e_{33}\tilde{\epsilon}_r + e_{13}(\tilde{\epsilon}_\theta + \tilde{\epsilon}_z) + \tilde{\epsilon}_{33}\tilde{E}_r,\ \tilde{D}_z = 2e_{15}\tilde{\epsilon}_{rz} + \tilde{\epsilon}_{11}\tilde{E}_z
\end{aligned} \tag{18}$$

we have the differential–difference analogue of Eq. (15) in the form

$$\begin{aligned}
\frac{\mathrm{d}\mathscr{E}^h}{\mathrm{d}t} &= \rho \sum_{\bar{\omega}_h} r\hbar_1\hbar_2 \left[\frac{\partial \tilde{u}_1}{\partial t}\frac{\partial^2 \tilde{u}_1}{\partial t^2} + \frac{\partial \tilde{u}_2}{\partial t}\frac{\partial^2 \tilde{u}_2}{\partial t^2} \right]\\
&+ \sum_{\omega_h^+} \bar{r}h_1h_2 \left[\frac{\partial \tilde{\epsilon}_r}{\partial t}\tilde{\sigma}_r + \frac{\partial \tilde{\epsilon}_\theta}{\partial t}\tilde{\sigma}_\theta + \frac{\partial \tilde{\epsilon}_z}{\partial t}\tilde{\sigma}_z + \frac{\partial \tilde{\epsilon}_{rz}}{\partial t}(2\tilde{\sigma}_{rz}) \right]\\
&+ \sum_{\omega_h^+} \bar{r}h_1h_2 \left[\tilde{E}_r \frac{\partial \tilde{D}_r}{\partial t} + \tilde{E}_z \frac{\partial \tilde{D}_z}{\partial t} \right],
\end{aligned} \tag{19}$$

where

$$\begin{aligned}
\mathscr{E}^h &= \frac{\rho}{2} \sum_{\bar{\omega}_h} r\hbar_1\hbar_2 \left[\left(\frac{\mathrm{d}\tilde{u}_1}{\mathrm{d}t} \right)^2 + \left(\frac{\mathrm{d}\tilde{u}_2}{\mathrm{d}t} \right)^2 \right] + \frac{1}{2} \sum_{\omega_h^+} \bar{r}h_1h_2 \Big[c_{33}\tilde{\epsilon}_r^2 + c_{11}(\tilde{\epsilon}_\theta^2 + \tilde{\epsilon}_z^2)\\
&\quad + 2c_{13}(\tilde{\epsilon}_\theta + \tilde{\epsilon}_z)\tilde{\epsilon}_r + 2c_{12}\tilde{\epsilon}_r\tilde{\epsilon}_\theta + 2c_{44}\tilde{\epsilon}_{rz}^2 + \epsilon_{33}\tilde{E}_r^2 + \epsilon_{11}\tilde{E}_z^2 \Big].
\end{aligned} \tag{20}$$

Applying grid formulas for summation by parts [28,29] from Eq. (19) we derive the differential–difference analogue of the conservation law (15)

$$\begin{aligned}
\frac{\mathrm{d}\mathscr{E}^h}{\mathrm{d}t} &= \sum_{\bar{\omega}_h} r\hbar_1\hbar_2 \left[f_1 \frac{\tilde{u}_1}{\partial t} + f_2 \frac{\tilde{u}_2}{\partial t} \right] + \sum_{\bar{\omega}_{h_1}} r\hbar_1 \left(\tilde{\sigma}_{rz}\frac{\tilde{u}_1}{\partial t} + \tilde{\sigma}_z \frac{\tilde{u}_2}{\partial t} \right) \Bigg|_{j=0}^{j=M}\\
&+ \sum_{\bar{\omega}_{h_2}} r\hbar_2 \left(\tilde{\sigma}_r \frac{\tilde{u}_1}{\partial t} + \tilde{\sigma}_{rz}\frac{\tilde{u}_2}{\partial t} \right) \Bigg|_{i=0}^{i=N} + \sum_{\bar{\omega}_h} r\hbar_1\hbar_2 \tilde{\varphi} \frac{\partial f_3}{\partial t}.
\end{aligned} \tag{21}$$

Now, using Eq. (21), we can easily derive differential–difference analogues of the equations for motion of the electroelastic medium, the Maxwell equation, and *natural* boundary conditions (9) and (10). The reader may consult [22], where such a procedure were explained for one-dimensional problems, for details.

The second stage of the construction of difference schemes requires the time discretisation. As a result of such discretisation, we obtain the following difference scheme:

$$\begin{aligned} &\rho y_{\bar{t}t} = \Lambda_1(y,g,\mu) + F_1, \\ &\rho g_{\bar{t}t} = \Lambda_2(y,g,\mu) + F_2, \\ &\Lambda_3(y,g,\mu) = F_3, \end{aligned} \tag{22}$$

where functions y, g and μ are discrete-argument functions that give approximations to the functions $u_r(r,z,t)$, $u_z(r,z,t)$ and $\varphi(r,z,t)$ respectively. The difference operators Λ_i, $i=1,2,3$ and right hand sides F_i, $i=1,2,3$ in Eq. (22) are defined as follows

$$\Lambda_1(y,g,\mu) =$$

$$\begin{cases}
\frac{1}{r}\left(\bar{r}\frac{\bar{\sigma}_r+\bar{\sigma}_r^{+1_z}}{2}\right)_r + \frac{1}{r}\left(\bar{r}\bar{\sigma}_{rz} + \bar{r}^{(+1)}\bar{\sigma}_{rz}^{(+1_r)}\right)_z - \frac{\bar{\sigma}_\theta+\bar{\sigma}_\theta^{(+1_r)}+\bar{\sigma}_\theta^{(+1_z)}+\bar{\sigma}_\theta^{(+1,+1)}}{4r} & (r,z)\in\omega_h, \\
\frac{1}{r}\left(\bar{r}\bar{\sigma}_r^{(+1_z)}\right)_r + \frac{1}{r}\frac{2}{h_2}\left(\frac{\bar{r}\bar{\sigma}_{rz}^{(+1_z)}+\bar{r}^{(+1)}\bar{\sigma}_{rz}^{(+1,+1)}}{2}\right) - \frac{\bar{\sigma}_\theta^{(+1_z)}+\bar{\sigma}_\theta^{(+1,+1)}}{2r} & (r,z)\in\gamma_1, \\
\frac{1}{r}\left(\bar{r}\bar{\sigma}_r\right)_r - \frac{1}{r}\frac{2}{h_2}\left(\frac{\bar{r}\bar{\sigma}_{rz}+\bar{r}^{(+1)}\bar{\sigma}_{rz}^{(+1_r)}}{2}\right) - \frac{\bar{\sigma}_\theta+\bar{\sigma}_\theta^{(+1_r)}}{2r} & (r,z)\in\gamma_2, \\
\frac{1}{r}\bar{r}^{(+1)}\left(\bar{\sigma}_{rz}^{(+1_r)}\right)_z + \frac{1}{r}\frac{2}{h_1}\bar{r}^{(+1)}\left(\frac{\bar{\sigma}_r^{(+1_r)}+\bar{\sigma}_r^{(+1,+1)}}{2}\right) - \frac{\bar{\sigma}_\theta^{(+1_r)}+\bar{\sigma}_\theta^{(+1,+1)}}{2r} & (r,z)\in\gamma_3, \\
\frac{1}{r}\bar{r}\left(\bar{\sigma}_{rz}\right)_z - \frac{1}{r}\frac{2}{h_1}\bar{r}\left(\frac{\bar{\sigma}_r+\bar{\sigma}_r^{(+1_z)}}{2}\right) - \frac{\bar{\sigma}_\theta+\bar{\sigma}_\theta^{(+1_z)}}{2r} & (r,z)\in\gamma_4, \\
\frac{1}{r}\frac{2}{h_1}\bar{r}^{(+1)}\bar{\sigma}_r^{(+1,+1)} + \frac{1}{r}\frac{2}{h_2}\bar{r}^{(+1)}\bar{\sigma}_{rz}^{(+1,+1)} - \frac{\bar{\sigma}_\theta^{(+1,+1)}}{r} & (r,z)\in\gamma_{13}, \\
\frac{1}{r}\frac{2}{h_1}\bar{r}^{(+1)}\bar{\sigma}_r^{(+1_r)} - \frac{1}{r}\frac{2}{h_2}\bar{r}^{(+1)}\bar{\sigma}_{rz}^{(+1_r)} - \frac{\bar{\sigma}_\theta^{(+1_r)}}{r} & (r,z)\in\gamma_{23}, \\
-\frac{1}{r}\frac{2}{h_1}\bar{r}\bar{\sigma}_r^{(+1_z)} + \frac{1}{r}\frac{2}{h_2}\bar{r}\bar{\sigma}_{rz}^{(+1_z)} - \frac{\bar{\sigma}_\theta^{(+1_z)}}{r} & (r,z)\in\gamma_{14}, \\
-\frac{1}{r}\frac{2}{h_1}\bar{r}\bar{\sigma}_r - \frac{1}{r}\frac{2}{h_2}\bar{r}\bar{\sigma}_{rz} - \frac{\bar{\sigma}_\theta}{r} & (r,z)\in\gamma_{24},
\end{cases}$$

$$\Lambda_2(y,g,\mu)=\begin{cases}\frac{1}{r}\left(\bar{r}\frac{\bar{\sigma}_{rz}+\bar{\sigma}_{rz}^{+1_z}}{2}\right)_r+\frac{1}{r}\left(\bar{r}\bar{\sigma}_z+\bar{r}^{(+1)}\bar{\sigma}_z^{(+1_r)}\right)_z & (r,z)\in\omega_h.\\ \frac{1}{r}\left(\bar{r}\bar{\sigma}_{rz}^{(+1_z)}\right)_r+\frac{1}{r}\frac{2}{h_2}\left(\frac{\bar{r}\bar{\sigma}_z^{(+1_z)}+\bar{r}^{(+1)}\bar{\sigma}_z^{(+1,+1)}}{2}\right) & (r,z)\in\gamma_1,\\ \frac{1}{r}\left(\bar{r}\bar{\sigma}_{rz}\right)_r-\frac{1}{r}\frac{2}{h_2}\left(\frac{\bar{r}\bar{\sigma}_z+\bar{r}^{(+1)}\bar{\sigma}_z^{(+1_r)}}{2}\right)-\frac{\bar{\sigma}_\theta^{+}\bar{\sigma}_\theta^{(+1_r)}}{2r} & (r,z)\in\gamma_2,\\ \frac{1}{r}\bar{r}^{(+1)}\left(\bar{\sigma}_z^{(+1_r)}\right)_z+\frac{1}{r}\frac{2}{h_1}\bar{r}^{(+1)}\left(\frac{\bar{\sigma}_{rz}^{(+1_r)}+\bar{\sigma}_{rz}^{(+1,+1)}}{2}\right) & (r,z)\in\gamma_3,\\ \frac{1}{r}\bar{r}\left(\bar{\sigma}_z\right)_z-\frac{1}{r}\frac{2}{h_1}\bar{r}\left(\frac{\bar{\sigma}_{rz}+\bar{\sigma}_{rz}^{(+1_z)}}{2}\right) & (r,z)\in\gamma_4,\\ \frac{1}{r}\frac{2}{h_2}\bar{r}^{(+1)}\bar{\sigma}_z^{(+1,+1)}+\frac{1}{r}\frac{2}{h_1}\bar{r}^{(+1)}\bar{\sigma}_{rz}^{(+1,+1)} & (r,z)\in\gamma_{13},\\ \frac{1}{r}\frac{2}{h_1}\bar{r}^{(+1)}\bar{\sigma}_{rz}^{(+1_r)}-\frac{1}{r}\frac{2}{h_2}\bar{r}^{(+1)}\bar{\sigma}_z^{(+1_r)} & (r,z)\in\gamma_{23},\\ -\frac{1}{r}\frac{2}{h_1}\bar{r}\bar{\sigma}_{rz}^{(+1_z)}+\frac{1}{r}\frac{2}{h_2}\bar{r}\bar{\sigma}_z^{(+1_z)} & (r,z)\in\gamma_{14},\\ -\frac{1}{r}\frac{2}{h_1}\bar{r}\bar{\sigma}_{rz}-\frac{1}{r}\frac{2}{h_2}\bar{r}\bar{\sigma}_z & (r,z)\in\gamma_{24},\end{cases}$$

$$\Lambda_3(y,g,\mu)=\begin{cases}\frac{1}{r}\left(\bar{r}\frac{\bar{D}_r+\bar{D}_r^{+1_z}}{2}\right)_r+\frac{1}{r}\left(\bar{r}\bar{D}_z+\bar{r}^{(+1)}\bar{D}_z^{(+1_r)}\right)_z & (r,z)\in\omega_h,\\ \frac{1}{r}\left(\bar{r}\bar{D}_r^{(+1_z)}\right)_r+\frac{1}{r}\frac{2}{h_2}\left(\frac{\bar{r}\bar{D}_z^{(+1_z)}+\bar{r}^{(+1)}\bar{D}_z^{(+1,+1)}}{2}\right) & (r,z)\in\gamma_1,\\ \frac{1}{r}\left(\bar{r}\bar{D}_r\right)_r-\frac{1}{r}\frac{2}{h_2}\left(\frac{\bar{r}\bar{D}_z+\bar{r}^{(+1)}\bar{D}_z^{(+1_r)}}{2}\right) & (r,z)\in\gamma_2,\\ \mu & (r,z)\in\bar{\omega}_h/\\ & (\omega_h\cup\gamma_1\cup\gamma_2),\end{cases}$$

$$F_3=\begin{cases}f_3 & (r,z)\in\omega_h\cup\gamma_1\cup\gamma_2,\\ 0 & (r,z)\in\bar{\omega}_h/(\omega_h\cup\gamma_1\cup\gamma_2),\end{cases}$$

$$F_1 = f_1 + \begin{cases} 0 & (r,z) \in \omega_h, \\ -\frac{2}{h_2} p_{rt}^{(0)} & (r,z) \in \gamma_1, \\ \frac{2}{h_2} p_{rt}^{(1)} & (r,z) \in \gamma_2, \\ -\frac{2}{h_1} p_{r}^{(0)} & (r,z) \in \gamma_3, \\ \frac{2}{h_1} p_{rt}^{(1)} & (r,z) \in \gamma_4, \\ -\frac{2}{h_1} p_{r}^{(0)} - \frac{2}{h_2} p_{rt}^{(0)} & (r,z) \in \gamma_{13}, \\ -\frac{2}{h_1} p_{r}^{(0)} + \frac{2}{h_2} p_{rt}^{(1)} & (r,z) \in \gamma_{23}, \\ \frac{2}{h_1} p_{r}^{(1)} - \frac{2}{h_2} p_{rt}^{(0)} & (r,z) \in \gamma_{14}, \\ \frac{2}{h_1} p_{r}^{(1)} + \frac{2}{h_2} p_{rt}^{(1)} & (r,z) \in \gamma_{24}, \end{cases}$$

$$F_2 = f_2 + \begin{cases} 0 & (r,z) \in \omega_h, \\ -\frac{2}{h_2} p_{z}^{(0)} & (r,z) \in \gamma_1, \\ \frac{2}{h_2} p_{z}^{(1)} & (r,z) \in \gamma_2, \\ -\frac{2}{h_1} p_{zt}^{(0)} & (r,z) \in \gamma_3, \\ \frac{2}{h_1} p_{zt}^{(1)} & (r,z) \in \gamma_4, \\ -\frac{2}{h_1} p_{zt}^{(0)} - \frac{2}{h_2} p_{z}^{(0)} & (r,z) \in \gamma_{13}, \\ -\frac{2}{h_1} p_{zt}^{(0)} + \frac{2}{h_2} p_{z}^{(1)} & (r,z) \in \gamma_{23}, \\ \frac{2}{h_1} p_{zt}^{(1)} - \frac{2}{h_2} p_{z}^{(0)} & (r,z) \in \gamma_{14}, \\ \frac{2}{h_1} p_{zt}^{(1)} + \frac{2}{h_2} p_{z}^{(1)} & (r,z) \in \gamma_{24}. \end{cases}$$

The fully discrete approximations of the state equations follow immediately from Eq. (18)

$$\begin{aligned} &\bar{\sigma}_r = c_{33}\bar{\epsilon}_r + c_{13}(\bar{\epsilon}_\theta + \bar{\epsilon}_z) - e_{33}\bar{E}_r, \quad \bar{\sigma}_\theta = c_{13}\bar{\epsilon}_r + c_{11}\bar{\epsilon}_\theta + c_{12}\bar{\epsilon}_z - e_{13}\bar{E}_r, \\ &\bar{\sigma}_z = c_{13}\bar{\epsilon}_r + c_{12}\bar{\epsilon}_\theta + c_{11}\bar{\epsilon}_z - e_{13}\bar{E}_r, \quad \bar{\sigma}_{rz} = c_{44}\bar{\epsilon}_{rz} - e_{15}\bar{E}_z, \\ &\bar{D}_r = \bar{E}_r + e_{33}\bar{\epsilon}_r + e_{13}(\bar{\epsilon}_\theta + \bar{\epsilon}_z), \quad \bar{D}_z = \epsilon_{11}\bar{E}_z + 2e_{15}\bar{\epsilon}_{rz}, \end{aligned} \tag{23}$$

where

$$\bar{E}_r = \frac{1}{2}\left(\mu_{\bar{r}} + \mu_{\bar{r}}^{(-1_z)}\right), \qquad \bar{E}_z = \frac{1}{2}\left(\mu_{\bar{z}} + \mu_{\bar{z}}^{(-1_r)}\right),$$

$$\bar{\epsilon}_r = \frac{1}{2}\left(y_{\bar{r}} + y_{\bar{r}}^{(-1_z)}\right), \qquad \bar{\epsilon}_\theta = \frac{1}{4\bar{r}}\left(y + y^{(-1_r)} + y^{(-1_z)} + y^{(-1,-1)}\right),$$

$$\bar{\epsilon}_z = \frac{1}{2}\left(g_{\bar{z}} + g_{\bar{z}}^{(-1_r)}\right), \qquad 2\bar{\epsilon}_{rz} = \frac{1}{2}\left(y_{\bar{z}} + y_{\bar{z}}^{(-1_r)} + g_{\bar{r}} + g_{\bar{r}}^{(-1_z)}\right).$$

The first pair of initial conditions is approximated exactly

$$y(r,z,0) = u_r^{(0)}(r,z), \qquad g(r,z,0) = u_z^{(0)}(r,z). \tag{24}$$

The second pair of initial conditions is approximated by the central difference derivative with subsequent elimination of the (-1)st fictitious time-layer by using the first two equation of the system (22) for $t = 0$. The result is

$$\rho y_t = \rho u_r^{(1)} + \frac{\tau}{2}(F_1 + \Lambda_1(y,g,\mu)), \qquad \rho g_t = \rho u_z^{(1)} + \frac{\tau}{2}(F_2 + \Lambda_2(y,g,\mu)). \tag{25}$$

6. Bound on the energy functional in nonstationary coupled models

When expressed as a finite set of equations, mathematical conservation laws may be only an approximate reflection of the real-world situation. In order to guarantee an adequateness of such a reflection, it is important to obtain an upper bound estimate for the energy functional. On the one hand, such estimates may be used as a measure of model applicability to specific practical problems. On the other hand, such estimates play a fundamental role in investigating system stability. In this section we derive such an estimate from the energy balance Eq. (15).

Integrating Eq. (15) with respect to t from zero to t_1 $(0 < t_1 \leqslant T)$ and taking into account conditions (9) and (10) we have

$$\mathscr{E}(t_1) = \mathscr{E}(0) + \int_0^{t_1} \int \int_\Omega r\left[\frac{\partial D_r}{\partial t}E_r + \frac{\partial D_z}{\partial t}E_z\right] \mathrm{d}\Omega\, \mathrm{d}t$$

$$+ \int_0^{t_1}\int_{R_0}^{R_1} r\left[\frac{\partial u_r}{\partial t}\bigg|_{Z_1} p_{rt}^{(1)} - \frac{\partial u_r}{\partial t}\bigg|_{Z_0} p_{rt}^{(0)}\right] \mathrm{d}r\, \mathrm{d}t$$

$$
+\int_0^{t_1}\int_{R_0}^{R_1} r\left[\frac{\partial u_z}{\partial t}\bigg|_{Z_1} p_z^{(1)} - \frac{\partial u_z}{\partial t}\bigg|_{Z_0} p_z^{(0)}\right] \mathrm{d}r\,\mathrm{d}t
$$

$$
+\int_0^{t_1}\int_{Z_0}^{Z_1} r\left[\frac{\partial u_r}{\partial t}\bigg|_{R_1} p_r^{(1)} - \frac{\partial u_r}{\partial t}\bigg|_{R_0} p_r^{(0)}\right] \mathrm{d}z\,\mathrm{d}t
$$

$$
+\int_0^{t_1}\int_{Z_0}^{Z_1} r\left[\frac{\partial u_z}{\partial t}\bigg|_{R_1} p_{zt}^{(1)} - \frac{\partial u_z}{\partial t}\bigg|_{R_0} p_{zt}^{(0)}\right] \mathrm{d}z\,\mathrm{d}t
$$

$$
+\int_0^{t_1}\int\int_{\Omega}\left[f_1\frac{\partial u_r}{\partial t} + f_2\frac{\partial u_z}{\partial t}\right] \mathrm{d}\Omega\,\mathrm{d}t. \tag{26}
$$

Now we have to estimate additives in the right-hand side of Eq. (26). As an example, we consider

$$
\begin{aligned}
I_1 &= \int_0^{t_1}\int_{R_0}^{R_1} r\left[\frac{\partial u}{\partial t}\bigg|_{Z_1} p_{rt}^{(1)} - \frac{\partial u}{\partial t}\bigg|_{Z_0} p_{rt}^{(0)}\right] \mathrm{d}r\,\mathrm{d}t \\
&= \int_{R_0}^{R_1} r\Big\{\big[p_{rt}^{(1)}(r,t_1)u_r(r,Z_1,t_1) - p_{rt}^{(1)}(r,0)u_r(r,Z_1,0)\big] \\
&\quad -\big[p_{rt}^{(0)}(r,t_1)u_r(r,Z_0,t_1) - p_{rt}^{(0)}(r,0)u_r(r,Z_0,0)\big]\Big\}\,\mathrm{d}r \\
&\quad +\int_0^{t_1}\int_{R_0}^{R_1} r\left\{u_r(r,Z_0,t)\frac{\partial p_{rt}^{(0)}}{\partial t} - u_r(r,Z_1,t)\frac{\partial p_{rt}^{(1)}}{\partial t}\right\} \mathrm{d}r\,\mathrm{d}t = I_1^{(1)} + I_1^{(2)},
\end{aligned} \tag{27}
$$

where

$$
\begin{aligned}
I_1^{(1)} &= \int_{R_0}^{R_1} r\Big\{\big[p_{rt}^{(1)}(r,t_1)u_r(r,Z_1,t_1) - p_{rt}^{(1)}(r,0)u_r(r,Z_1,0)\big] \\
&\quad -\big[p_{rt}^{(0)}(r,t_1)u_r(r,Z_0,t_1) - p_{rt}^{(0)}(r,0)u_r(r,Z_0,0)\big]\Big\}\,\mathrm{d}r, \\
I_1^{(2)} &= \int_0^{t_1}\int_{R_0}^{R_1} r\left\{u_r(r,Z_0,t)\frac{\partial p_{rt}^{(0)}}{\partial t} - u_r(r,Z_1,t)\frac{\partial p_{rt}^{(1)}}{\partial t}\right\} \mathrm{d}r\ \ \mathrm{d}t.
\end{aligned}
$$

Using the Cauchy–Schwartz inequality and the ϵ-inequality [28,29,22] we get

$$I_1^{(1)} \leqslant M_5^{(1)} \int_{R_0}^{R_1} \left[|u_r(r, Z_0, t_1)|^2 + |u_r(r, Z_1, t_1)|^2 \right] \mathrm{d}r$$

$$+ M_5^{(2)} \int_{R_0}^{R_1} \left[|u_r(r, Z_0, 0)|^2 + |u_r(r, Z_1, 0)|^2 \right] \mathrm{d}r$$

$$+ M_1^{(3)} \int_{R_0}^{R_1} \left[|p_{rt}^{(0)}(r, t_1)|^2 + |p_{rt}^{(1)}(r, t_1)|^2 + |p_{rt}^{(0)}(r, 0)|^2 + |p_{rt}^{(1)}(r, 0)|^2 \right] \mathrm{d}r. \tag{28}$$

We apply the functional analysis technique based on embedding theorems [28,32] in order to obtain estimates of the first two terms in the RHS of Eq. (28):

$$\int_{R_0}^{R_1} \left[|u_r(r, Z_0, t_1)|^2 + |u_r(r, Z_1, t_1)|^2 \right] \mathrm{d}r$$

$$\leqslant M_6^{(1)} \int\int_{\Omega} \left(\frac{\partial u_r}{\partial z} \right)^2 \bigg|_{t=t_1} \mathrm{d}\Omega, \quad \int_{R_0}^{R_1} \left[|u_r(r, Z_0, 0)|^2 + |u_r(r, Z_1, 0)|^2 \right] \mathrm{d}r$$

$$\leqslant M_6^{(2)} \int\int_{\Omega} \left(\frac{\partial u_r}{\partial z} \right)^2 \bigg|_{t=0} \mathrm{d}\Omega.$$

Let $M_5^{(i)} M_6^{(i)} = M_1^{(i)}$, $i = 1, 2$. Then from Eq. (28) we get

$$I_1^{(1)} \leqslant M_1^{(1)} \int\int_{\Omega} \left(\frac{\partial u_r}{\partial z} \right)^2 \bigg|_{t=t_1} \mathrm{d}\Omega + M_1^{(2)} \int\int_{\Omega} \left(\frac{\partial u_r}{\partial z} \right)^2 \bigg|_{t=0} d\Omega$$

$$+ M_1^{(3)} \int R_0^{R_1} \left[|p_{rt}^{(0)}(r, t_1)|^2 + |p_{rt}^{(1)}(r, t_1)|^2 + |p_{rt}^{(0)}(r, 0)|^2 + |p_{rt}^{(1)}(r, 0)|^2 \right] \mathrm{d}r. \tag{29}$$

In a similar way, we transform the other three additives of the right-hand side of Eq. (26).

Estimates of integrals of $I_1^{(2)}$-type can also be performed by applying the ϵ-inequality and embedding theorems. For example, it is not difficult to obtain that

$$I_1^{(2)} \leqslant M_1^{(4)} \int_0^{t_1} \left(\frac{\partial u_r}{\partial z} \right)^2 \mathrm{d}t + M_1^{(5)} \int_0^{t_1} \int_{R_0}^{R_1} \left[\left(\frac{\partial p_{rt}^{(0)}}{\partial t} \right)^2 + \left(\frac{\partial p_{rt}^{(1)}}{\partial t} \right)^2 \right] \mathrm{d}r \, \mathrm{d}t. \qquad (30)$$

We take into account Eqs. (29) and (30) in estimating Eq. (26) and apply the following lemma on integral inequality:

Lemma 6.1 ([11]). *Let function* $I(t) \geqslant 0$ $(0 \leqslant t \leqslant T)$ *is continuous, differentiable and such that it satisfies the following inequality*

$$I(t_2) \leqslant I(t_1) + M \int_{t_1}^{t_2} I(t) \, \mathrm{d}t + N \int_{t_1}^{t_2} \sqrt{I(t)} \, \mathrm{d}t$$

$$\textit{for any } 0 \leqslant t_1 \leqslant t_2 \leqslant T \ (M > 0, \ N \geqslant 0).$$

Then

$$\sqrt{I(t)} \leqslant \sqrt{I(0)} \, \exp\left(\frac{M}{2} t \right) + \frac{N}{M} \left(\exp\left(\frac{M}{2} t \right) - 1 \right).$$

As a result, from Eq. (26) we derive the following estimate

$$\begin{aligned}
\mathscr{E}(t_1) \leqslant M_1 \mathscr{E}(0) + M_2 \Bigg\{ & \int_{R_0}^{R_1} \left[\sum_{i,j=0}^{1} \left(|p_{rt}^{(i)}(r, t_j)|^2 + |p_z^{(i)}(r, t_j)|^2 \right) \right] \mathrm{d}r \\
& + \int_{Z_0}^{Z_1} \left[\sum_{i,j=0}^{1} \left(|p_r^{(i)}(r, t_j)|^2 + |p_{zt}^{(i)}(r, t_j)|^2 \right) \right] \mathrm{d}z \\
& + \int_0^{t_1} \int_{R_0}^{R_1} \sum_{i=0}^{1} \left[\left(\frac{\partial p_{rt}^{(i)}}{\partial t} \right)^2 + \left(\frac{\partial p_z^{(i)}}{\partial t} \right)^2 \right] \mathrm{d}r \, \mathrm{d}t \\
& + \int_0^{t_1} \int_{Z_0}^{Z_1} \sum_{i=0}^{1} \left[\left(\frac{\partial p_r^{(i)}}{\partial t} \right)^2 + \left(\frac{\partial p_{zt}^{(i)}}{\partial t} \right)^2 \right] \mathrm{d}z \, \mathrm{d}t \\
& + \int_0^{t_1} \int \int_{\Omega} r(f_1^2 + f_2^2) \Bigg\} \mathrm{d}\Omega \, \mathrm{d}t,
\end{aligned} \qquad (31)$$

where the time variable is taken at $t = t_1$ if $j = 1$ and at $t = t_0 = 0$ if $j = 0$. Note that in inequality (31) we have taken into account that

$$\frac{\partial D_r}{\partial t} = \frac{\partial D_z}{\partial t} = 0$$

(see [22] for details).

Now we have to estimate the total energy of the electro-mechanical system at the initial moment of time, using initial conditions (7), (8). The main difficulty (as it was in the one-dimensional case), consists of obtaining an estimate of electric-field-energy integral.

First, let us estimate the quantity

$$\int\int_{\Omega} r\left[E_r^2 + E_z^2\right]\big|_{t=0}\,\mathrm{d}\Omega.$$

It is straightforward to get the following identity

$$\int\int_{\Omega} r[D_rE_r + D_zE_z]\,\mathrm{d}\Omega = \int\int_{\Omega} r\lambda(E_r + E_z)\,\mathrm{d}\Omega, \tag{32}$$

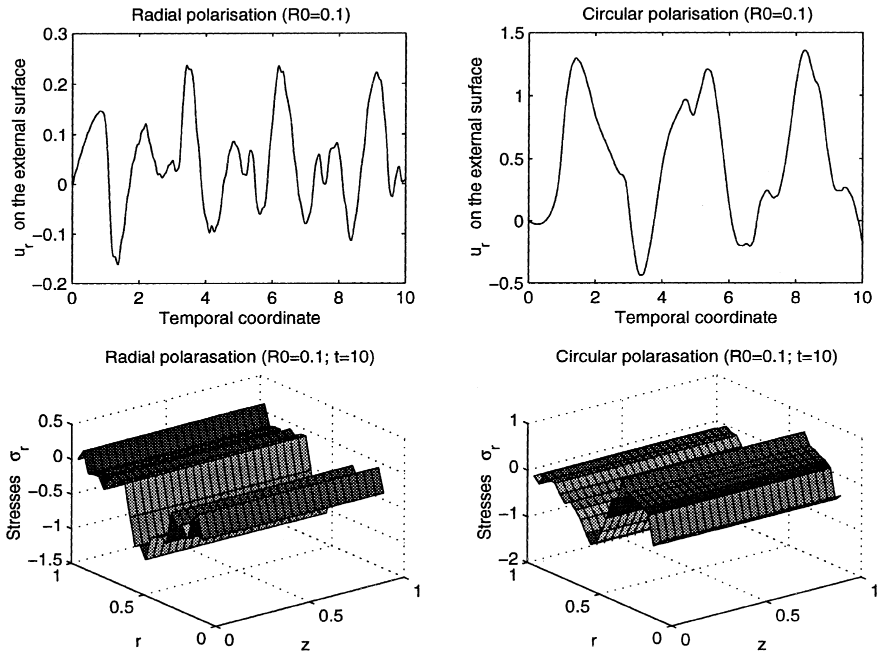

Fig. 1. Displacements and radial stresses in an "infinitely-long" thick cylinder ($l = 0.9$, $a = 0.001$).

where the quantity λ is defined by the relationships

$$\frac{\partial\lambda}{\partial r}+\frac{\partial\lambda}{\partial z}=f_3, \qquad \lambda(R_0,z,t)=\lambda(r,Z_0,t)=0. \tag{33}$$

Taking into account state Eq. (4) from Eq. (32) we obtain

$$\min\{c_1,c_2\}\int\int_{\Omega} r(E_r^2+E_z^2)\big|_{t=0}\,\mathrm{d}\Omega \leqslant c_1\int\int_{\Omega} rE_r^2\big|_{t=0}\,\mathrm{d}\Omega$$

$$+\,c_2\int\int_{\Omega} rE_z^2\big|_{t=0}\,\mathrm{d}\Omega \leqslant M_3\int\int_{\Omega} r\big[\lambda^2+\epsilon_r^2+\epsilon_\theta^2+\epsilon_z^2+\epsilon_{rz}^2\big]\big|_{t=0}\,\mathrm{d}\Omega,$$

where c_1, c_2 are constants that depend on properties of the electro-elastic medium. Therefore

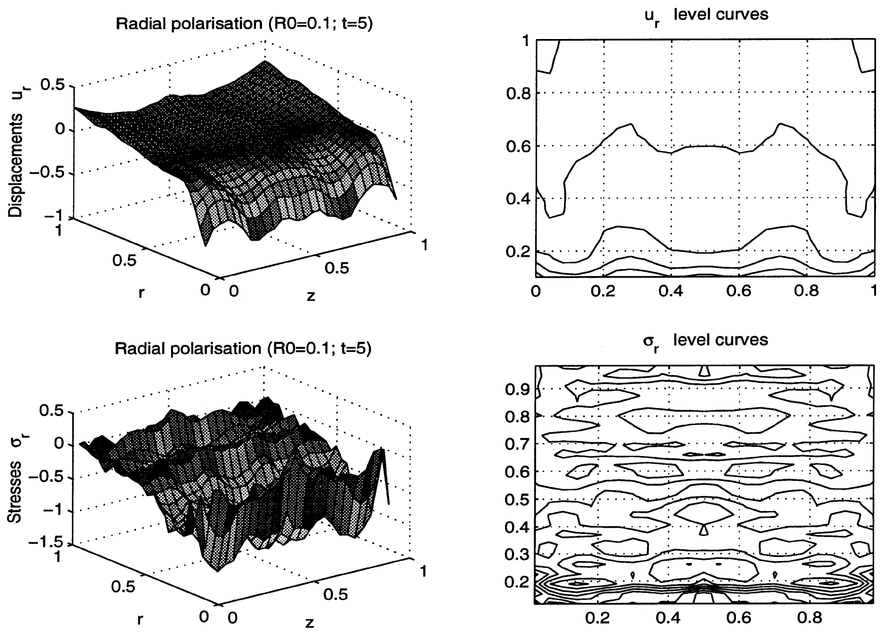

Fig. 2. Displacements and radial stresses in a finite-length thick cylinder with radial preliminary polarisation ($l=0.9$, $a=1$).

$$\mathscr{E}(0) \leqslant \frac{\rho}{2} \int\int r\Big[(u_r^{(1)})^2 + (u_z^{(1)})^2\Big] \, \mathrm{d}\Omega + \frac{1}{2} \int\int_{\Omega} r\big[c_{33}\epsilon_r^2 + c_{11}(\epsilon_\theta^2 + \epsilon_z^2)$$

$$+ 2c_{13}(\epsilon_\theta\epsilon_r + \epsilon_z\epsilon_r) + 2c_{12}\epsilon_z\epsilon_\theta + 2c_{44}\epsilon_{rz}^2\big] \, \mathrm{d}\Omega + \frac{1}{2}\max\{\epsilon_{11}, \epsilon_{33}\}$$

$$\times \frac{M_3}{\min\{c_1, c_2\}} \int\int_{\Omega} r\big[\lambda^2 + \epsilon_r^2 + \epsilon_\theta^2 + \epsilon_z^2 + \epsilon_{rz}^2\big] \, \mathrm{d}\Omega, \tag{34}$$

where all additives in the right hand side of Eq. (34) are computed for $t = 0$.

Finally, if we take into account the condition of nonnegativity of the potential energy of deformation,

$$\delta_1 \sum_{i=1}^{4} \xi_i^2 \leqslant c_{33}\xi_1^2 + c_{11}(\xi_2^2 + \xi_3^2) + 2c_{13}(\xi_2\xi_1 + \xi_3\xi_1) + 2c_{12}\xi_3\xi_2$$

$$+ 2c_{44}\xi_4^2, \ \delta_1 > 0, \tag{35}$$

then from Eq. (31) we obtain an upper bound on the energy functional for the problem (1)–(11). Hence we have proved the following theorem.

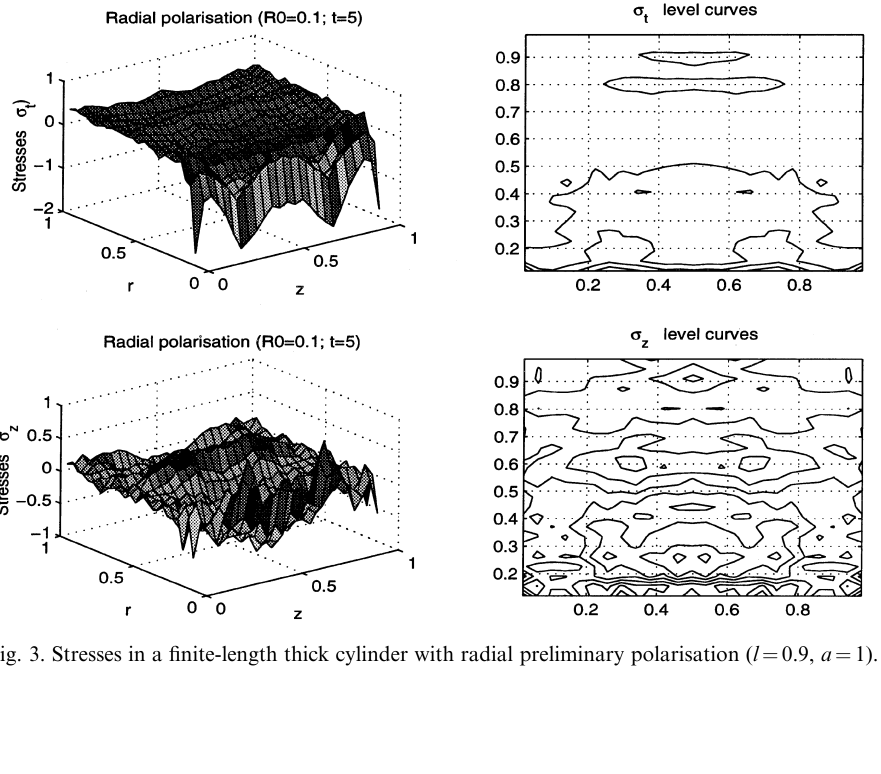

Fig. 3. Stresses in a finite-length thick cylinder with radial preliminary polarisation ($l = 0.9$, $a = 1$).

Theorem 6.1. *If the condition* (35) *holds, then the solution of the problems* (1)–(11) *satisfies the following energy bound*

$$\mathscr{E}(t_1) \leqslant M \Bigg\{ \rho \int\int_{\Omega} r\left[(u_r^{(1)})^2 + (u_z^{(1)})^2\right] \mathrm{d}\Omega + \int\int_{\Omega} r\big[c_{33}\epsilon_r^2 + c_{11}(\epsilon_\theta^2$$

$$+ \epsilon_z^2) + 2c_{13}(\epsilon_\theta + +\epsilon_z)\epsilon_r + 2c_{12}\epsilon_z\epsilon_\theta + 2c_{44}\epsilon_{rz}^2\big]|_{t=0}\, \mathrm{d}\Omega$$

$$+ \int_{R_0}^{R_1} \left[\sum_{i,j=0}^{1} \left(|p_{rt}^{(i)}(r,t_j)|^2 + |p_z^{(i)}(r,t_j)|^2 \right) \right] \mathrm{d}r$$

$$+ \int_{Z_0}^{Z_1} \left[\sum_{i,j=0}^{1} \left(|p_r^{(i)}(z,t_j)|^2 + |p_{zt}^{(i)}(z,t_j)|^2 \right) \right] \mathrm{d}z$$

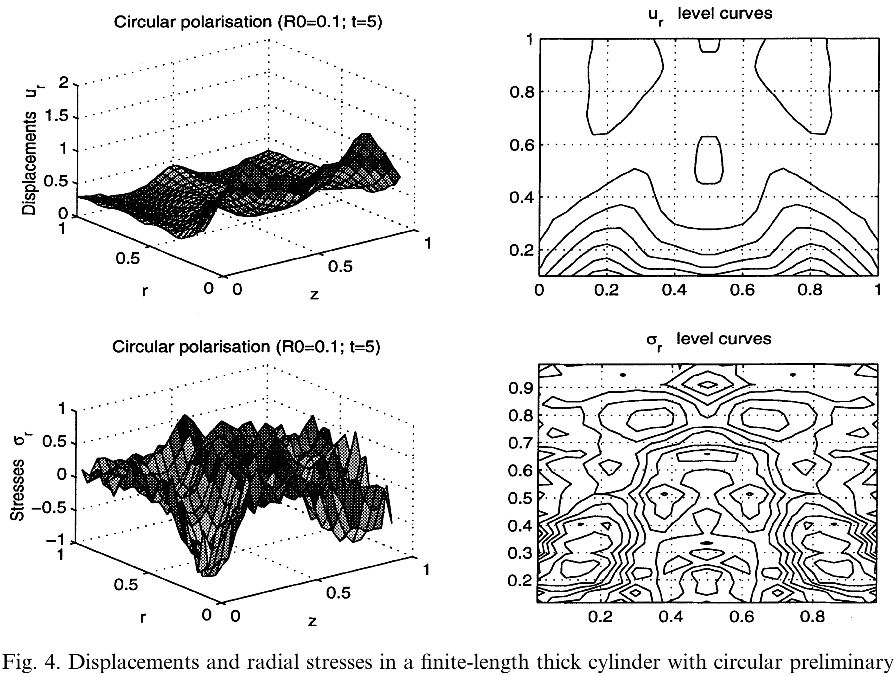

Fig. 4. Displacements and radial stresses in a finite-length thick cylinder with circular preliminary polarisation ($l = 0.9$, $a = 1$).

$$+\int_0^{t_1}\int_{R_0}^{R_1}\sum_{i=0}^{1}\left[\left(\frac{\partial p_{rt}^{(i)}}{\partial t}\right)^2+\left(\frac{\partial p_{z}^{(i)}}{\partial t}\right)^2\right]\mathrm{d}r\,\mathrm{d}t$$

$$+\int_0^{t_1}\int_{Z_0}^{Z_1}\sum_{i=0}^{1}\left[\left(\frac{\partial p_{r}^{(i)}}{\partial t}\right)^2+\left(\frac{\partial p_{zt}^{(i)}}{\partial t}\right)^2\right]\mathrm{d}z\,\mathrm{d}t+\int\int_{\Omega} r\lambda^2\big|_{t=0}\,\mathrm{d}\Omega$$

$$\left.+\int_0^{t_1}\int\int_{\Omega} r(f_1^2+f_2^2)\,\mathrm{d}\Omega\,\mathrm{d}t\right\}, \tag{36}$$

where $\mathscr{E}(t)$ is the total energy of the electro-mechanical system at time t, and λ is defined by the relationships (33).

Theorem 6.1 provides the basis for the investigation of stability of the electromechanical system. We will address the stability issues elsewhere.

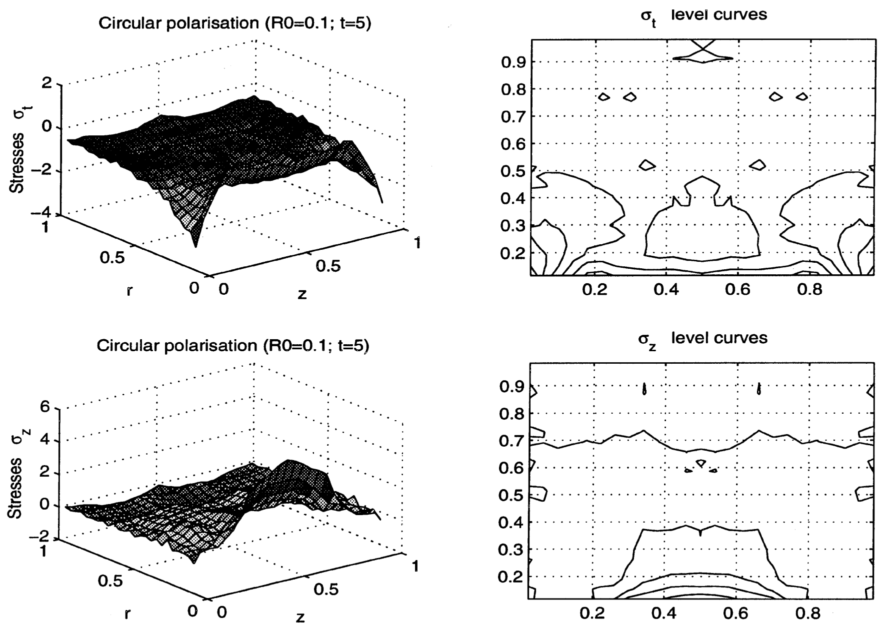

Fig. 5. Stresses in a finite-length thick cylinder with circular preliminary polarisation ($l = 0.9$, $a = 1$).

7. Numerical experiments

The important direction of piezoceramic application is connected with improved resolution and miniaturisation of technical devices. In such areas as biomedical imaging, nondestructive evaluation and hydroacoustics, devices produced from hollow piezoceramic cylinders or sphere may prove to be very useful [9,22].

We consider the results of modelling oscillations of hollow PZT-piezoceramic cylinders in the case when the potential difference $2V = 1$ is maintained on the "end-wall" of cylinders.

We note that, when the ratio of the cylinder thickness (l) to its height (H) is small ($l/H < R_1/H = a$), the results of computation with models (1)–(11) are in good agreement with the results for "infinitely"-long cylinders. Such results were obtained earlier with the one-dimensional model (see [22,24]).

One of the characteristics of practical interest is the dynamic of radial displacements on the external surface of cylinders. We conclude that, for thin cylinders poled radially, the magnitude of such displacements grows considerably faster (with the decrease of thickness) than for cylinders poled circularly. When thickness becomes larger, the magnitude of displacements of cylinders

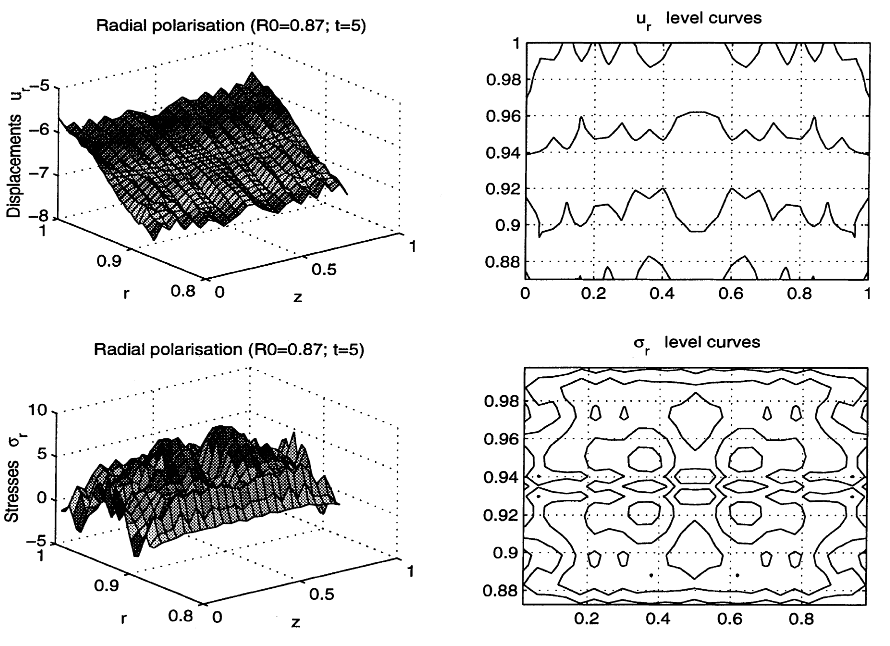

Fig. 6. Displacements and radial stresses in a finite-length thin cylinder with radial preliminary polarisation ($l = 0.13$, $a = 1$).

with circular preliminary polarisation typically exceeds the magnitude of displacements for cylinders with radial preliminary polarisation. As an example we present the results of computations for a thick cylinder with $l = 0.9$ (Fig. 1). Other examples may be found in Ref. [21].

For finite-length cylinders, the use of two-dimensional models is essential. The error in computation of displacements on the external surface of cylinders with $l = 0.13$ and $H = 1$ may exceed 27% for cylinders with radial preliminary polarisation and 16% for cylinders with circular preliminary polarisation.

Figs. 2 and 3 present the results of computations for cylinders with radial preliminary polarisation ($l = 0.9$). We compare these results for the same cylinder poled circularly (see Figs. 4 and 5). We observe, that for thick cylinders, the circular preliminary polarisation produces larger amplitudes of oscillations on the external surfaces of cylinders. Axial stresses in cylinders poled circularly may essentially exceed axial stresses in cylinders with radial preliminary polarisation.

For thin cylinders, even the qualitative picture becomes completely different (see Figs. 6 and 7 for results on cylinders poled radially and Figs. 8 and 9 for results on cylinders with circular preliminary polarisation). In the thin-cylinder case, both characteristics, displacements and stresses, are essentially larger for cylinders with radial preliminary polarisation. The results on quantitative

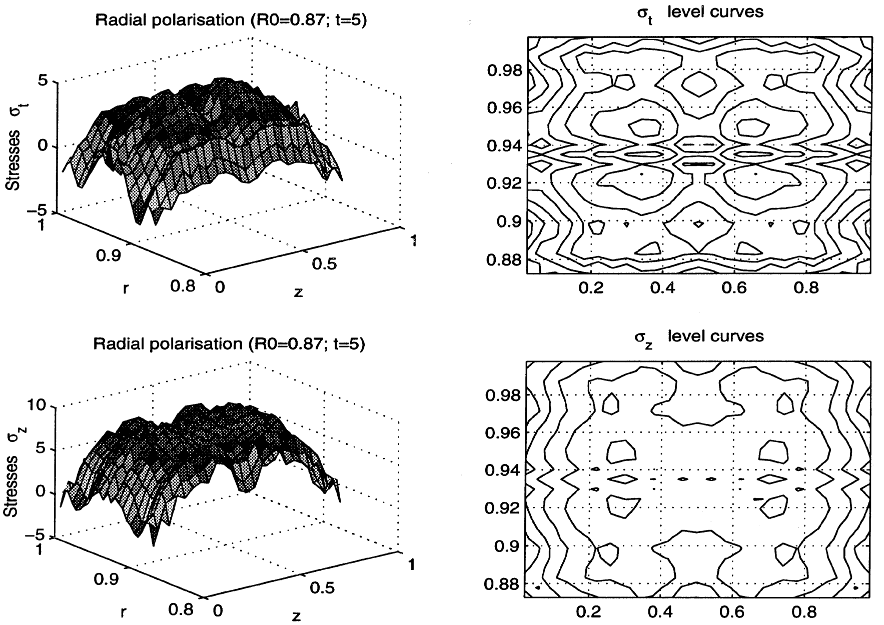

Fig. 7. Stresses in a finite-length thin cylinder with radial preliminary polarisation ($l = 0.13$, $a = 1$).

estimates of such characteristics are an important prerequisite for the successful design of acoustic radiators, transducers, sensors and many other technical devices constructed from piezoceramic.

8. Concluding remarks

Compared to pure elastic situations, the coupling elastic and electric fields, as well as anisotropy of physical properties of piezoelectric materials (for example, elastic, piezoelectric and dielectric moduli of piezoceramic), essentially complicates the analysis of wave phenomena that take place in piezoelectric bodies. Even the one-dimensional problem in the nonstationary case, presents a mathematically challenging and physically important problem. In order to obtain a plausible picture of the coupling phenomenon, methods for the solution of dynamical problems of electroelasticity may not always be based on thickness averaging of mechanical components of electro-elastic fields and the subsequent use of the Kirchoff–Lave-type hypothesis. Such averaging techniques, successful in the theory of plates and shells applied to elastic bodies, may not provide an appropriate tool in coupled field theory. It is often more

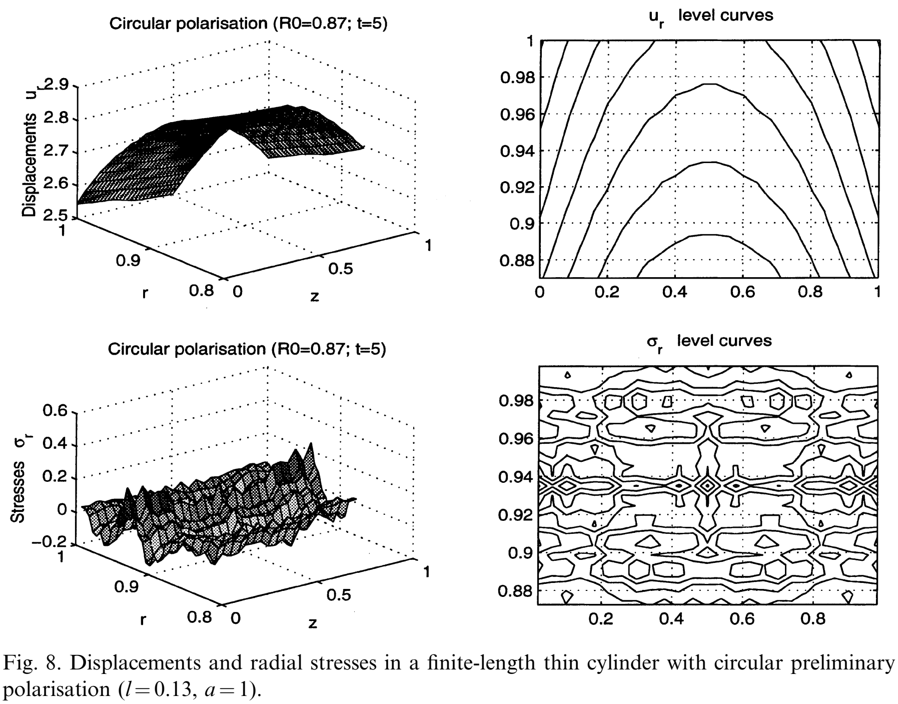

Fig. 8. Displacements and radial stresses in a finite-length thin cylinder with circular preliminary polarisation ($l = 0.13$, $a = 1$).

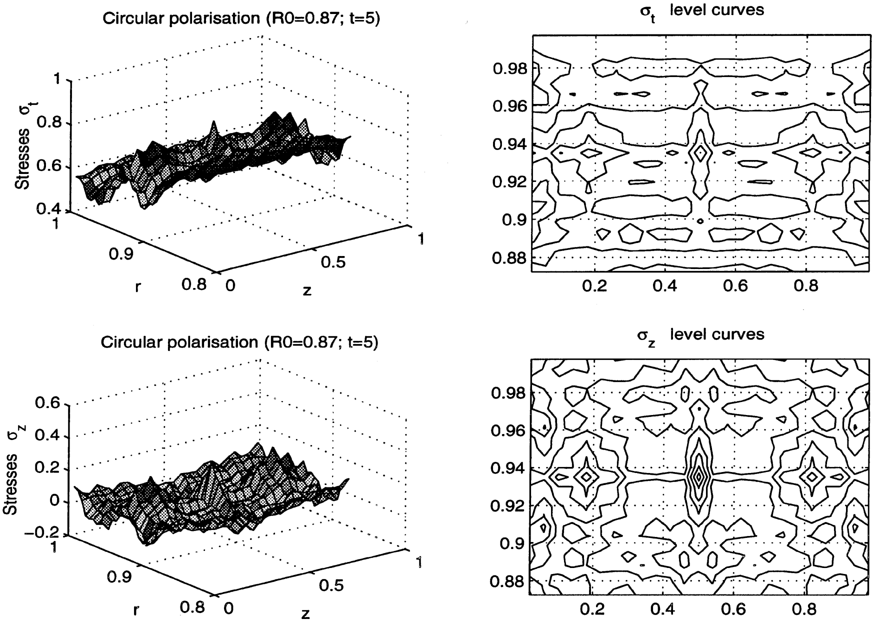

Fig. 9. Stresses in a finite-length thin cylinder with circular preliminary polarisation ($l = 0.13$, $a = 1$).

reasonable to directly apply an effective numerical technique to the original nonstationary coupled problem.

Piezoelectricity gives just one example where the coupling phenomenon between two different physical fields has to be dealt with in the early stage of mathematical modelling for the successful design of various technical devices. The directions of coupled field theory are virtually unexhaustable, with thermoelasticity, pyroelectricity, electrootics, magnetoelasticity, magnetooptics giving just few additional examples. In the final analysis, it is clear that there is no single field in nature that acts on its own. Of course, in some cases it may be unreasonable and/or impractical to include the information about other fields. Then we may limit ourselves to a specific (and, perhaps, very good) approximation. Nevertheless, in understanding many physical, chemical and biological phenomena, it is important to include additional information about different interrelated components of these phenomena into our approximations. The improvement of such approximations is intrinsically connected with the physical parameterisation of mathematical models. In order to gain a more penetrating insight into the coupled field theory concepts, including those of piezoelectricity, we have to look deep down inside the structure of the material [6,7]. Therefore, only a blend of the methods and techniques of mathematics, physics and material sciences can provide the necessary tools for the investigation of physical phenomena in finite structures.

Acknowledgements

The work was partially supported by grant USQ-PTRP 179389. I am deeply grateful to the School of Mathematics at the University of South Australia, where a part of this work was made, for their hospitality. I also would like to thank Anne Fuller for her helpful assistance at the final stage of preparation of this paper.

References

[1] E.E. Antonova, P.P. Silvester, Finite elements for piezoelectric vibrations with open electric boundaries, IEEE Trans. Ultrason., Ferroelect., Freq. Contr. 44 (3) (1997) 548–556.
[2] A. Ballato, Piezoelectricity: Old effect, new thrusts, IEEE Trans. Ultrason., Ferroelect. 42 (5) (1995) 916.
[3] D.A. Berlincourt, D.R. Curran, H. Jaffe, Piezoelectric and piezomagnetic materials and their function in transducers, in: W.P. Mason (Ed.), Physical Acoustics, vol. 1A, Academic Press, New York and London, 1964, pp. 204–236.
[4] L.F. Brown, Ferroelectric polymers: Current and future ultrasonic applications, Proceedings of the IEEE Ultrasonic Symposium, 1992, pp. 539–550.
[5] G.R. Buchanan, J. Peddieson Jr., Vibration of infinite piezoelectric cylinders with anisotropic properties using cylindrical finite elements, IEEE Trans. Ultrason., Ferroelect., Freq. Contr. 38 (3) (1991) 291–301.
[6] R.C. Buchanan (Ed.), Ceramic Materials for Electronics: Processing, Properties, and Applications, Marcel Dekker, New York, 1991.
[7] Long-Qing Chen et al. (Eds.), Mathematics of Microstructure Evolution, Proceedings in Applied Mathematics, vol. 90, SIAM and MMMS, Philadelphia, 1996.
[8] E. Dieulesaint, D. Royer, Elastic Waves in Solids: Applications to Signal Processing, Wiley, Chichester, New York, 1980.
[9] J.T. Fielding et al., Characterization of PZT hollow-sphere transducers, Proceedings of the IX IEEE International Symposium on Applications of Ferroelectrics, 1994, pp. 202–205.
[10] E. Fukada, Poiseuille medal award lecture: Piezoelectricity of biopolymers, Biorheology 32 (1995) 1995.
[11] S.K. Godunov, Equations of Mathematical Physics, Nauka, Moscow, 1980.
[12] T.R. Gururaja, Piezoelectric transducers for medical ultrasonic imaging, American Ceramic Society Bulletin 73 (5) (1994) 50–55.
[13] T. Ikeda, Fundamentals of Piezoelectricity, Oxford University Press, Oxford, 1990.
[14] Y. Kagawa, T. Tsuchiya, T. Kawashima, Finite element simulation of piezoelectric vibrator gyroscopes, IEEE Trans. Ultrason., Ferroelect., Freq. Contr. 43 (4) (1996) 120–509.
[15] Y. Kawawa, T. Tsuchiya, G. Furukawa, Finite element simulation of dynamic responses of piezoelectric actuators, J. Sound and Vibration 191 (4) (1996) 519–528.
[16] J.S. Lee, Boundary element method for electroelastic interaction in piezoceramics, Eng. Anal. with Boundary Elements 15 (4) (1995) 321–328.

[17] R. Le Letty, F. Claeyssen, R. Bossut, Combined finite element-normal mode expansion methods in electroelasticity and their application to piezoactive motors, Int. J. Numer. Methods Eng. 40 (18) (1997) 3385–3395.
[18] R. Lerch, Simulation of piezoelectric devices by two- and three-dimensional finite elements, IEEE Trans. Ultrason., Ferroelect., Freq. Contr. 37 (3) (1990) 233–243.
[19] P. Lu, O. Mahrenholtz, A variational boundary element formulation for piezoelectricity, Mech. Res. Commun. 21 (6) (1994) 605–615.
[20] R.V.N. Melnik, Existence and uniqueness theorems of the generalised solutions for a class of non-stationary problems of coupled electroelasticity, S. Mathematics (Iz. VUZ), Allerton Press 35 (4) (1991) 24–32.
[21] R.V.N. Melnik, M.N. Moskalkov, Difference schemes for and analysis of approximate solutions of two-dimensional nonstationary problems in coupled electroelasticity, Differential Equations 27 (7) (1991) 1220–1230 (from Plenum Publishing Corporation/Consultants Bureau, New York, 1992, pp. 860–867).
[22] R.V.N. Melnik, The stability condition and energy estimate for non-stationary problems of coupled electroelasticity, Math. and Mech. of Solids 2 (2) (1997) 153–180.
[23] R.V.N. Melnik, Intelligent structures and coupling in mathematical models: examples from dynamic electroelasticity, Proceedings of the IEEE ICPADM '97, Seoul, Korea, 1997, Vol. 2, 995–998.
[24] R.V.N. Melnik, Convergence of the operator-difference scheme to generalized solutions of a coupled field theory problem, Journal of Difference Equations and Applications, to be published.
[25] M.N. Moskalkov, Investigation of a difference scheme for the solution of the sound radiator problem for cylindric piezovibrators, Differential Equations 22 (7) (1986) 1220–1226.
[26] W. Nowacki, Electromagnetic Effects in Solids, Mir Publishers, Moscow, 1986.
[27] C.Z. Rosen, B.V. Hiremath, R. Newnham (Eds.), Piezoelectricity, N.Y. American Institute of Physics, 1992.
[28] A.A. Samarskii, Theorie der Differenzenverfahren, (Series: Mathematik und ihre Anwendungen in Physik und Technik), Aufl. Leipzig: Academische Verlagsgesellschaft Geest and Portig, 1984.
[29] A.A. Samarskii, E.S. Nikolaev, Numerical Methods for Grid Equations, Birkhauser, Basel, 1989.
[30] M. Shashkov, S. Steinberg, Conservative Finite Difference Methods on General Grids, CRC Press, Boca Raton, 1995.
[31] S. Takahashi, Ferroelectric Ceramics, in: N. Setter, E.L. Colla (Eds.), Birkhauser, Basel, 1993, pp. 349–362.
[32] V.A. Trenogin, Functional Analysis, Nauka, Moscow, 1993.
[33] A.O. Vatulyan, V.L. Kublikov, Boundary element method in electroelasticity, Boundary Elements Commun. 6 (2) (1995) 59–61.